Available online at www.sciencedirect.com
ScienceDirect
Journal of Power Sources 182 (2008) 462–468
JOURNAL OF POWER SOURCES
www.elsevier.com/locate/jpowsour

Corrosion of metallic stack components in molten carbonates: Critical issues and recent findings

Stefano Frangini *

Department TER, ENEA CRE Casaccia, Via Anguillarese 301, 00060 Rome, Italy

Received 23 October 2007; received in revised form 22 November 2007; accepted 24 November 2007
Available online 5 December 2007

Abstract

The influence of stainless steel hardware corrosion on molten carbonate fuel cell (MCFC) cell performance decay modes is briefly reviewed. Emphasis has been given to the cathode-side corrosion of the separator plate, which is the most critical performance-limiting factor due to the growth of thick oxide scales with a poor electrical conductivity causing relevant cell voltage losses on prolonged operations. Voltage decay is related to loss of electrolyte by reaction with the growing oxide scale and to the onset of an ohmic resistance at the point of contact between the corroded separator plate and the cathode. The increase of ohmic resistance over the time is the major cause of voltage decay with the currently used austenitic 316L and 310S stainless steels. A short literature survey is presented in the second part of this paper reporting on the most promising alternative corrosion-resistant alloys or protective coatings suitable for fabrication of long-term stable cathode-side MCFC separator plates.

Keywords: Molten carbonate fuel cell; Stainless steel corrosion; Separator plate; Voltage decay; Electrolyte loss; Ohmic resistance

1. Introduction

Molten carbonate fuel cell (MCFC) is nowadays the most promising fuel cell technology for high-efficiency cogeneration of electricity and heat with a minimal environmental impact. In fact, a low NO_x emission results from use of reformed methane or coal gas as a fuel at approximately 600–680 °C. This temperature level is optimal for a large use of commonly available metal sheets that can be stamped in low-cost processes for fabrication of cell and stack components. More exactly, MCFC can be defined as a stainless steel-based technology in which the stainless steels contribute for more than 50% in weight to the total composition of a fuel cell stack (Fig. 1). Conventional austenitic 316L and 310S stainless steels are widely used for present MCFC metallic hardware both having acceptable high-temperature strength and corrosion resistance [1].

Metallic corrosion represents a critical decay mode that affects both performance and lifetime of MCFC cells. Corrosion rates are dependent on a large number of variables such as temperature, gas composition and pressure, moisture and impurities. In particular, CO_2 is a strong corrosive agent as it controls the melt acidity, which in turn determines the extent of corrosion. Thus, as the operating pressure of MCFC stacks increases, the faster hardware corrosion may result in accelerated voltage losses (in a 5-bar 20 kW stack, for instance, untolerable voltage loss rates of 3–4 times higher than in atmospheric systems have been reported [2]).

In general, the corrosion of the separator plate is the most critical for the cell performance as this component is in direct contact with the corrosive molten salt [3]. The state-of-the-art MCFC stack life has now surpassed the 25,000 h in commercial-size plants operating at ambient pressure. At this stage of product development, the cathode-side endurance of stainless steel separator plate is emerging as a major impediment for additional significant stack lifetime (voltage decay rate needs to be at or lower than 2 mV 1000 h^{-1} to get a 40,000 h of stack life, as required to compete with other distributed power generation systems). Therefore, it is strongly believed that the use of corrosion-resistant alloys or protective coatings is likely one of the key strategies for high-performance separator plates. The still high cost of the current MCFC systems are mostly due to the conventional peripherical equipments rather than to the fuel cell stack. Approximately, the fuel cell stack contributes for only one-third to the overall system cost. Therefore, it is felt

* Tel.: +39 06 30483138; fax: +39 06 30483327.
E-mail address: frangini@casaccia.enea.it.

0378-7753/$ – see front matter © 2007 Elsevier B.V. All rights reserved.
doi:10.1016/j.jpowsour.2007.11.100

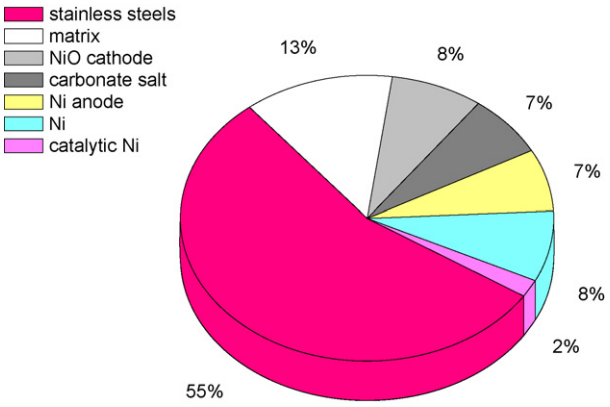

Fig. 1. Typical composition (wt%) of a molten carbonate fuel cell stack (after Ref. [17]).

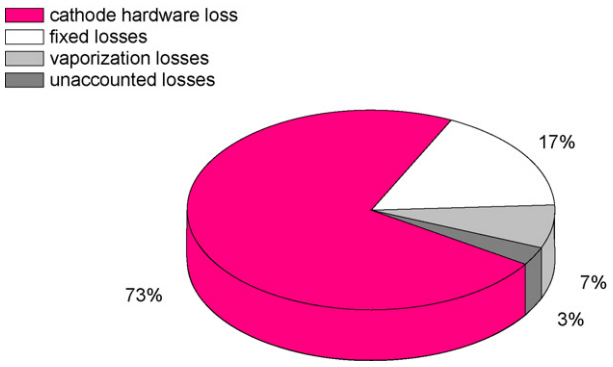

Fig. 2. Electrolyte loss inventory of a spent MCFC stack (data refer to the analysis of 2MW Santa Clara Demo power plant [4]).

that the use of high-cost alloys or coatings for critical metallic components may be tolerable on the overall system cost.

Because of the complex environment of a MCFC, corrosion of the separator plate takes place in three characteristic regions: the cathode and the anode areas, where the metal is covered with a thin molten carbonate film under highly oxidizing and reducing/carburizing gas conditions, respectively, and the so-called wet-seal region, where the metal is in contact with a thick carbonate layer under variable gas composition. These different chemical conditions can interact in a very complex way with the metal surface leading to various forms of dangerous corrosive attack [3]. In the first part of this paper, the most critical aspects of the cell degradation performances related to corrosion are being reviewed and discussed separately for each cell area. This part will be followed by a survey of the most recent literature on alternate cathode-side materials as molten carbonate corrosion in this area is widely recognized as the most critical performance-limiting factor.

2. Molten carbonate corrosion: critical issues

2.1. Cathode area

Cell degradation performance by separator plate (SP) corrosion in this area is mainly related to the growth of a corrosion product layer that consumes electrolyte material and increases the ohmic resistance between SP and electrode.

Detailed analysis of electrolyte loss mechanisms has shown that almost 70% of the total electrolyte loss is due to the cathode-side hardware corrosion (Fig. 2) [4]. In modern MCFC plants, this loss is tolerable and corresponds to about 20% of the beginning-of-life, BOL, inventory on a projected time of 40,000 h, whereas the contribution due to external hardware corrosion (manifolds, end plates and so forth) and to internal anode-side separator plate corrosion is very low (about 5% of BOL inventory) [5].

In detail, electrolyte loss is due to the formation of insoluble Li-containing corrosion products such as $LiFeO_2$ and K, Na-containing soluble corrosion products such as K_2CrO_4 (in Li/K electrolyte) or Na_2CrO_4 (in Li/Na electrolyte). The corrosion scale consists of three distinct layers, two oxide layers and one metal layer. The outer oxide layer is prevalently composed of $LiFeO_2$, which forms for the reaction between the initially formed Fe_2O_3 and Li_2CO_3. The $LiFeO_2$ layer is followed by an internal compact and protective Cr-containing layer growing by internal oxidation mechanisms. Finally, the innermost metal layer is depleted of chromium resulting from the soluble chromate formation under the oxidizing gas conditions of the cathodic compartment. The chromate formation causes preferential loss of K_2CO_3 or Na_2CO_3 with a further voltage loss as the chromate deeply changes the wetting behavior of the melt driving its creeping out from the porous cathode electrode structure (creepage loss) [5].

Due to higher Cr content in the 310S steel, total electrolyte consumption may become larger than that of 316L (Fig. 3) [5]. It is to be noted that loss rates are also very dependent on the geometry design of the separator plate. Decreasing contacting surface area of the separator plate contributes significantly to reduce BOL loss below 25% by strong attenuation of electrolyte creepage.

Both corrosion and creepage loss rates are proportional to the square root of time. These rates are consistent with well-known diffusion-limited corrosion laws and indicate that electrolyte loss and creepage are fast at an early stage and much slower later [6] (see Figs. 4 and 5). The corrosion and creepage alter

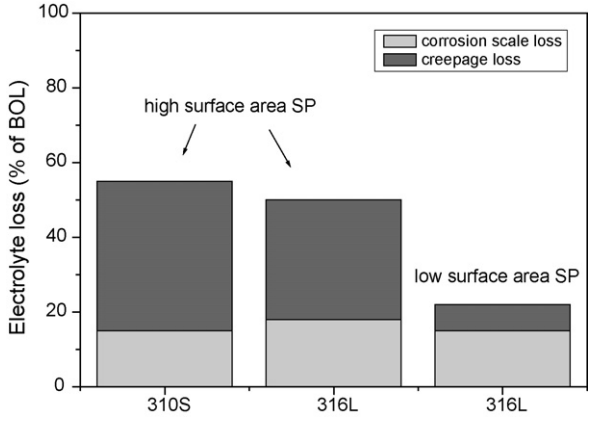

Fig. 3. Electrolyte loss projected on 40,000 h: <25% BOL is achievable with a low surface area separator plate that minimizes creepage loss.

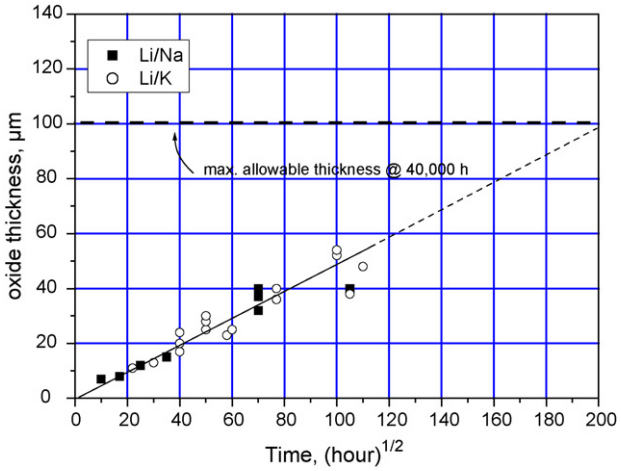

Fig. 4. Time dependence of oxide scale thickness for a 316L stainless steel separator plate in Li/K and Li/Na carbonate electrolytes (after Ref. [6]).

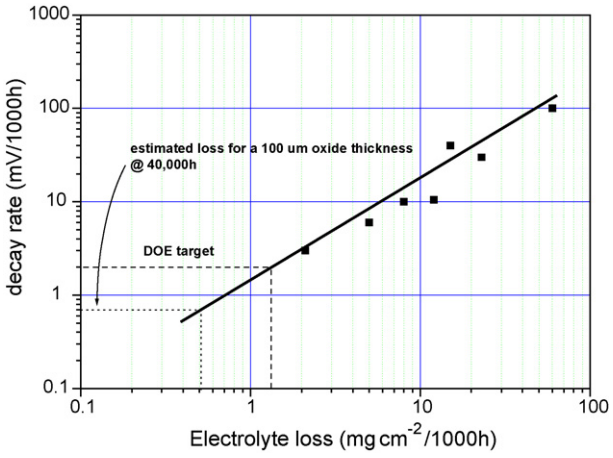

Fig. 6. Relationship between electrolyte loss and voltage decay rate (after Ref. [7]).

the electrolyte distribution within the cell porous components resulting in an increase of electrode polarization, matrix ionic resistance and even gas reactant cross-over in case of matrix drying. Quantitative relationships between electrolyte loss and voltage decay have been build based on practical experience data [7] as shown in Fig. 6. Thus, it can be predicted that a carbonate loss below 1.4 mg cm^{-2} 1000 h^{-1} is required to meet the target degradation rate of 2 mV 1000 h^{-1}. This target can be met with the current stainless steels. For instance, from Fig. 4 it is seen that for a 316L separator plate the scale thickness projected to 40,000 h corresponds almost exactly to the design goal (i.e., 100 μm), which is based on mechanical strength considerations (Fig. 4). The corresponding electrolyte loss estimated from Fig. 5 lies in the range 0.3–0.5 mg cm^{-2} 1000 h^{-1}, which means less than 1 mV 1000 h^{-1}.

With the currently used stainless steels, the voltage drop of a MCFC cell due to ohmic losses is a more stringent problem than electrolyte loss. The cell internal resistance is typically 0.3–0.4 Ω cm^2 and represents the sum of two main contributions: an ionic resistance due to the electrolyte matrix and an electronic resistance due to the corrosion layer resistance. Matrix contributes for more than the 70% to the total ohmic resistance, at BOL [8]. However, the increase rate of ionic resistance is very low (about 0.2–0.3 mV 1000 h^{-1} [7]) in contrast to that of the electronic resistance, which has been observed to increase parabolically with time alike to that of thickness change of corrosion layer causing significant voltage losses during long-time operations (see Fig. 7) [2,6,7]. As practicable countermeasure, pressing forces between 2 and 3 kg cm^{-2} are usually applied to the stacks to reduce the tendency to ohmic loss increases [9].

The electrical conductivity of the oxide scale is related to the alloy composition. Alloys with more than 20 wt% Cr show significantly higher ohmic resistance than that of alloys with less than 20 wt% Cr suggesting that the electrical conductivity is mostly determined by the inner Cr-containing corrosion layer [1]. The oxide formed on 316L has an initial lower interfacial

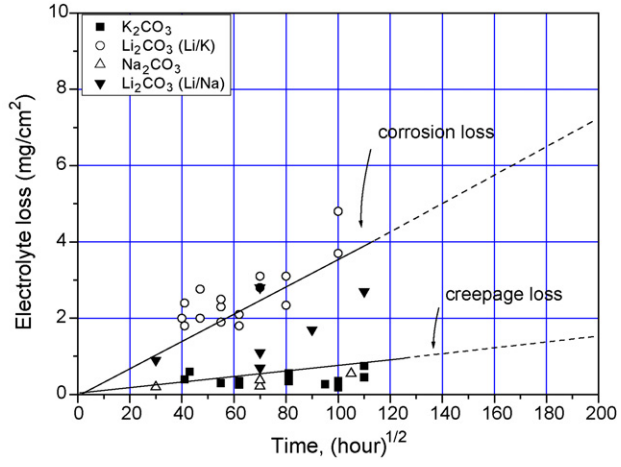

Fig. 5. Time dependence of electrolyte loss by corrosion and creepage mechanisms in Li/K and Li/Na carbonate electrolytes (after Ref. [6]).

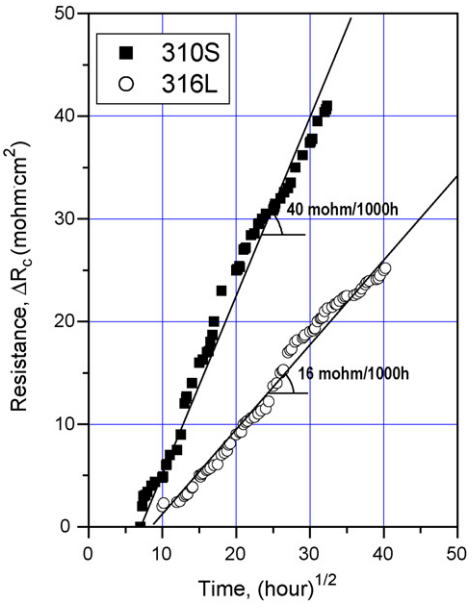

Fig. 7. Time dependence of ohmic contact resistance between oxide scales of 316L and 310S stainless steel separator plates and NiO cathode in LiK electrolyte (after Ref. [2]). The slopes indicate the ohmic increase rates.

resistance than that of 310S (0.05 vs. 0.20–0.25 Ω cm^2, at 650 °C [1]) as it contains more Fe that promotes the formation of higher conductive inner $FeCr_2O_4$ spinel layers. With 316L the initial ohmic drop can be estimated at only 7–8 mV at a current density of 0.15 A cm^{-2}, but it may increase to about as much as 90 mV after 40,000 h as calculated from Fig. 7, at a loss rate of 2 mV 1000 h^{-1}. On the other hand, the use of a 310S corresponds to a ca. 35 mV voltage loss at BOL and ca. 280 mV after 40,000 h (loss rate at 6 mV 1000 h^{-1} calculated from Fig. 7).

Because of less ohmic resistance and also of lower total electrolyte consumption, 316L steel is nowadays the preferred material for cathode-side separator plate by most developers. However, in pressurized systems, where corrosion is much more severe than in atmospheric ones, there is some advantage in using 310S to avoid excessive oxide scale thickening.

2.2. Anode area

The anode-side environment is much more corrosive for stainless steels than the cathode-side for the rapid formation of thick and non-protective multi-layered oxide scales [3,10]. In contrast, metals like Ni and Cu are thermodynamically stable in the anode gas atmosphere. For this reason, Ni clad stainless steels are usually applied for the realization of a corrosion-resistant anode-side separator plate. In these conditions, no growth of corrosion product takes place thus virtually eliminating both electrolyte loss and contact resistance in this area. However, in the anode atmosphere, these are the thermodynamic conditions for carburization reactions as the carbon activity is very high in this area ($a_c = 0.1$). Without Ni coating, carburization of steels would not be a problem, as carbon cannot penetrate through the oxidized surface to carburize the metallic substrate. Unfortunately, Ni coating has no sufficient barrier properties against the carbon transport due to high solubility (0.315 at.%) and diffusivity (2.68×10^{-10} cm^2 s^{-1}) of carbon in nickel at 650 °C [11]. This leads to formation of a deep carburization layer below the Ni coating along with diffused Cr carbide precipitation at grain boundaries of stainless steels resulting in Cr depletion and mechanical failure of the separator structure at long-term operations.

Another degradation process of the anode-side separator plate consists in the formation of small amounts of Cr-rich oxide particles at grain boundaries of the Ni layer due to outward Cr and Fe diffusion from the substrate stainless steel and inward oxygen diffusion. As the defect structure of Ni layer may act as an easy diffusion path, a virtually defect-free Ni layer is required for long-term MCFC operations. It has been clearly demonstrated that Ni clads are more dense than conventional electrolytic Ni coatings thus ensuring a better resistance against internal oxidation [12].

2.3. Wet-seal area

The edges of the separator plate are in direct contact with a thick molten carbonate layer to form a leak-free gas seal called wet-seal. Wet-seal corrosion is a particularly severe form of attack in a MCFC as it may lead to rapid deterioration and decline of cell performance [10]. Corrosion in this area takes place primarily due to establishment of various electrochemical couples (fuel–air, oxidant–air, oxidant–fuel) causing different corrosion rates in different areas of the wet-seal [13]. On the cathode-side corrosion rate of stainless steels is about two orders of magnitude lower than on anode-side. Stainless steels could be therefore used without significant problems in the cathode wet-seal, at least for short-term, whereas corrosion is unacceptably high at the anode-side, both at open circuit and under load. As only alumina-forming alloys are corrosion-resistant in such an environment, aluminum-diffusion coatings are generally applied to 316L and 310S before their use in wet-seal [10]. High-quality aluminization coatings are considered to provide an adequate corrosion-resistance, although there are some concerns about their long-term stability due to aluminum loss caused by its inward diffusion into the steel substrate [14].

In the current MCFC technology, various aluminizing methods are being applied such as ion vapor deposition, slurry painting, thermal spraying and cladding. In general, the aluminizing process must be accompanied by a heat treatment, which allows the establishment of a corrosion-resistant $LiAlO_2$ layer onto a high-melting point intermetallic aluminide compound formed during the heat treatment [10]. Recently, a low-cost Al-cladding method has been developed while still providing a high-quality coating as the protection intermetallic compound is formed *in situ* during stack start-up upon Al diffusion into the steel substrate in the temperature range between 500 and 650 °C [15].

3. Molten carbonate corrosion: literature survey

A survey on the molten carbonate corrosion of alternate materials for use as cathode-side hardware is presented based on the literature collected over the past 10 years. The survey covers corrosion rate data and electrical conductivity properties as they mainly affect MCFC performance degradation.

Recent studies focused on optimization of stainless steel composition to meet the stringent requirements for cathode-side separator. A great deal of systematic work on the effect of alloying elements on stainless steel performance has been conducted by German investigators [16–18]. As high-Cr steels (>20 wt%) such as 310S result in the formation of Cr_2O_3 insulating layers leading to both high electrolyte and ohmic losses, attention was mainly paid on steels with a moderate Cr content (between 15 and 20 wt%) that preferentially form conductive spinel layers. As Cr causes a decrease of the spinel electrical conductivity, the addition of transition elements was studied to further increase the p-type electrical conductivity of the $FeCr_2O_4$ spinel layer by substituting for Cr. It was found that Mn, Co and Ni are the most significant elements for the formation of good p-type conductive spinel oxides, whereas Si and Cr are mostly beneficial for good corrosion resistance [17]. From these works, it could be concluded that alloys with 16–18 Cr, 5–10 Ni, 4–10 Mn and/or Co, 3–6 Mo (wt%) should exhibit adequate corrosion resistance and low ohmic losses in long-term operations [16]. Based on these modelistic studies, two commercial manganese stainless steels were later subjected to investigation. A

Table 1
Chemical composition of various alternative metallic alloys proposed for cathode-side hardware, as compared with 316L and 310S state-of-the-art stainless steels

Alloy designation	Element (wt%)					
	Fe	Cr	Ni	Co	Mn	Others
Commercial alloys						
SS316L	bal.	16–18	11–14	–	<2	2–2.5Mo; 1Si
SS310S	bal.	24–26	19–22	–	<2	–
Mn Steel 1.3816	bal.	17–20	<1	–	17.5–20	–
Nitronic 50	bal.	20–23	11.5–13.5	–	4–6	1.5–3Mo
NKK	23–25	29–31	bal.	–	–	1Al; 0.03Y
Model alloys						
V152	bal.	17.6	3	5	12.2	3Mo; 0.5Si
FeCrCoMnMo	bal.	16.5	–	10	10	5Mo
FeCrTi	bal.	21	–	–	–	4Ti

high Mn-alloyed austenitic steel (DIN 1.3816 with a 17–20 wt% Mn) was found to promote formation of oxides with both good corrosion resistance and electrical conductivities [17]. Schoeler et al. also reported that a standard spinel-forming austenitic steel (i.e., Nitronic 50 produced by AK Steel Co., with a nominal composition of 20–23 Cr, 11–13 Ni, 4–6 Mn and 1.5–3 Mo) could also be a realistic alternative for its ability to form a protective corrosion scale with better conductive properties than that of 316L on a long-term basis [1].

A different approach was investigated by Nishina et al., who evaluated the effects of small additions of Al and/or Ti to a binary Fe–21Cr alloy [19]. As expected, it was found that a ternary Fe–21Cr–*X*Al ($X = 1$–4 wt%) was highly corrosion-resistant for the formation of an insulating $LiAlO_2$ film. On the other hand, the electrical conductivity of the corresponding ternary Fe–21Cr–*X*Ti alloys was only slightly higher than that of a 310S but with a much better corrosion resistance. This was ascribed to the formation of a Ti oxide film, which, differently from Al oxide, becomes a semi-conductor in a molten carbonate environment by Li-ion doping. As electrical conductivity is not much affected by increasing Ti additions, a ternary Fe–21Cr–4Ti was considered a best choice from both the point of view of corrosion resistance and electrical conductivity of the corroded scale. However, the effect of Ti on long-term conductivity was not reported.

Ni-based alloys were also studied but with less intensity than Fe-based alloys for their much higher costs. In general, commercial Ni-based alloys such as Inconel 718 and Inconel 625 are not suitable on the anode-side due to low oxygen partial pressures in which Ni remains metallic [20]. However, NKK Steel Corporation recently developed a new Ni-based alloy (45Ni–30Cr–24Fe–1Al–0.03Y, commonly known as NKK alloy) with good corrosion properties in both the cathode and anode sides of the separator plate [21]. Diverging values of electrical resistivity of NKK oxide scale were reported in [1] and [18]. As electrical conductivity is strongly affected by small additions of Al, it is suspected that the Al content of the NKK sample alloy used in [18] was significantly higher than 1 wt%.

Some research efforts were also devoted to the study of suitable corrosion-resistant coatings for the cathode-side of the separator plate, thus allowing the use of the current stainless steels. There are recent patent publications dealing with application of sol–gel coatings for corrosion protection of cathode-side hardware. US patent 2003/6,645,657 describes the behavior of thin conductive layers (thickness variable between 1 and 5 μm) of $LiCoO_2$ or Co-doped $LiFeO_2$ deposited on 316L stainless steel [22]. Coated stainless steel hardware showed significant thickness reduction of the corrosion layer resulting in a 30% less electrolyte consumption. Electrical conductivities of the coated steels were comparable to uncoated 316L. In a more recent US patent application (2005/0277015) sol–gel ceramic coatings of perovskite materials were preferred for corrosion protection for their high electrical conductivities and very low solubility in alkali melts, as compared to $LiCoO_2$ coatings [23]. More importantly, perovskite coatings were claimed to be also more dense and smooth and with better thermal compatibility with the steel substrates. Various perovskite of general formula $AMeO_3$, where A is lanthanum or a combination of lanthanum and strontium and Me is one or more of transition metals (Co, Mn, Cr, Fe) were deposited on 316L stainless steel. Steel coated with a LSC perovskite ($La_{0.8}Sr_{0.2}CoO_3$) layer was reported to

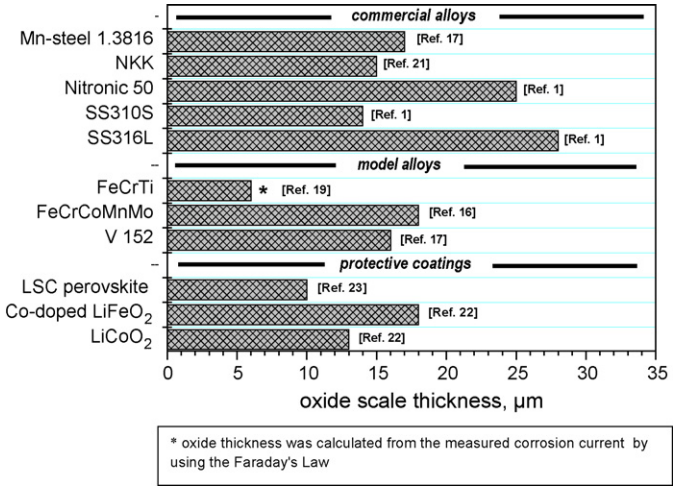

Fig. 8. Thickness of oxide scales on various metallic alloys and protective coatings proposed for cathode-side hardware after ca. 1000 h exposure in MCFC cathode environment, as compared with 316L and 310S state-of-the-art stainless steels.

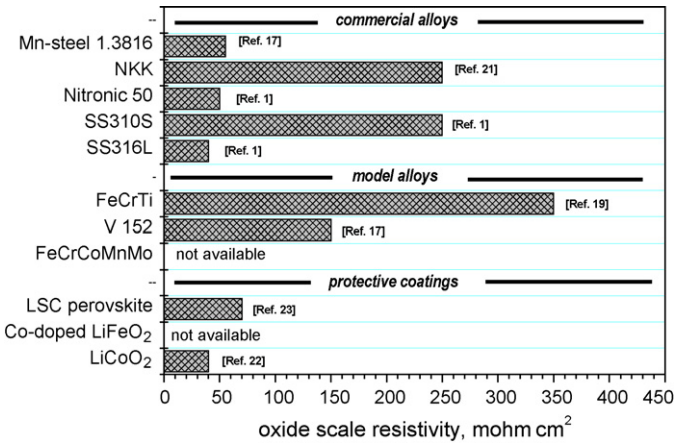

Fig. 9. Average ohmic resistance values in 500–1500 h time range for various metallic alloys and protective coatings proposed for cathode-side hardware, as compared with 316L and 310S state-of-the-art stainless steels.

exhibit very low corrosion with a contact resistance comparable to that of the uncoated steel. A 60% lower electrolyte loss was also reported.

Table 1 reports the chemical composition of the metallic alloys mentioned in this survey. The Figs. 8 and 9 summarize the cathode-side corrosion and, where available, also the electrical resistivity data, respectively. For NKK alloy the electrical resistivity reported in [1] is given.

As seen, several materials and coatings show a sufficiently low cathode-side corrosion to compete with the standard stainless steels. However, from this survey, it is also noted that ohmic resistance properties have not been sufficiently investigated on a long-term basis, although increase of contact resistance with time represents a power loss mechanism more important than the initial contact resistance value. Additional systematic studies on long-term electrical properties of candidate cathode-side materials are therefore desirable for a more significant comparison with the state-of-the-art stainless steels.

4. Conclusions

Separator plate corrosion is one of the life-limiting factors for MCFC cells. A concise overview on the effects of corrosion on cell performance has been given in the first part of this paper. Cathode-side corrosion of separator plate, currently made with stainless steels like 310S or 316L, is the most critical area for cell performance degradation due to a growing oxide scale with bad electrical conductivities. The ohmic resistance at points of contact between the oxide layer that forms on the separator plate surface and cathode is the major cause of voltage losses in long-term operations. On a projected 40,000 h time, ohmic voltage losses may become as high as 90 mV for 316L and more than 280 mV for 310S, both values being above the 80 mV target loss admitted for a 5-year system lifetime goal. The research in this area focuses on the search of new materials that combine the high corrosion resistance of 310S and the relatively high electrical conductivity of 316L oxide scale.

Analysis of the recent literature has shown a dominance of works aimed to optimize chemical composition of stainless steels for molten carbonate application. It has been demonstrated that manganese and nickel additions to stainless steels containing a moderate Cr content between 15–20 wt%, promote the formation of conductive spinel layers with a good compromise of corrosion resistance and electrical conductivity. In this context, commercial stainless steels containing manganese like Nitronic 50 and DIN 1.3816 could be realistic alternatives to 316L and 310S for fabrication of high-performance separator plates.

Moreover, the Ni-based NKK alloy shows also some promise for practical application in MCFC. The high-corrosion resistance of NKK alloy in both oxidizing and reducing gas conditions could in fact avoid the use of Ni protective coating on the anode-side separator plate, thus reducing the risks of mechanical breakdown caused by Ni layer delamination.

Finally, protective coatings based on conductive $LiCoO_2$ or perovskite materials may represent an interesting low-cost alternative to minimize cathode-side corrosion with the currently used stainless steels.

References

[1] A. Schoeler, T.D. Kaun, I. Bloom, M. Lanagan, M. Krumpelt, J. Electrochem. Soc. 147 (3) (2000) 916–921.
[2] A. Sano, in: J.R. Selman, I. Uchida, H. Wendt, D. Shores, T.F. Fuller (Eds.), Carbonate Fuel Cell Technology IV, Pennington, NJ, Electrochem. Soc. Proc. Ser. (1997) 51–65, PV 97-4.
[3] S. Frangini, in: A.C. Sequeira (Ed.), High Temperature Corrosion in Molten Salts, Trans Tech Publications Ltd., Switzerland, 2003, pp. 135–154.
[4] C.Y. Yuh, M. Farooque, H. Maru, in: I. Uchida, K. Hemmes, G. Lindbergh, D.A. Shores, J.R. Selman (Eds.), Carbonate Fuel Cell Technology V, Pennington, NJ, Electrochem. Soc. Proc. Ser. (1999) 189–201, PV 99-20.
[5] C.Y. Yuh, R. Johnsen, M. Farooque, H. Maru, in: D. Shores, H. Maru, I. Uchida, J.R. Selman (Eds.), Carbonate Fuel Cell Technology, Pennington, NJ, Electrochem. Soc. Proc. Ser. (1993) 158–170, PV 93-3.
[6] K. Yuasa, H. Kasai, T. Matsuo, A. Matsunaga, M. Hosaka, in: I. Uchida, K. Hemmes, G. Lindbergh, D.A. Shores, J.R. Selman (Eds.), Carbonate Fuel Cell Technology V, Pennington, NJ, Electrochem. Soc. Proc. Ser. (1999) 30–39, PV 99-20.
[7] A. Suzuki, T. Oota, Y. Masuda, C. Shoji, K. Yuasa, T. Matsuo, J.R. Selman, in: I. Uchida, H. Wendt, D. Shores, T.F. Fuller (Eds.), Carbonate Fuel Cell Technology IV, Pennington, NJ, Electrochem. Soc. Proc. Ser. (1997) 30–39, PV 97-4.
[8] Fuel Cell Handbook, fifth ed., EG&G Services Parsons Inc., U.S. Department of Energy, DE-AM26-99FT40575, October 2000.
[9] T. Nakayama, A. Sugawara, A. Miki, in: I. Uchida, K. Hemmes, G. Lindbergh, D.A. Shores, J.R. Selman (Eds.), Carbonate Fuel Cell Technology V, Pennington, NJ, Electrochem. Soc. Proc. Ser. (1999) 2–13, PV 99-20.
[10] C.Y. Yuh, R. Johnsen, M. Farooque, H. Maru, J. Power Sources 56 (1995) 1–10.
[11] P. Singh, in: C.J. Johnson, S.L. Pohlman (Eds.), Corrosion in Batteries and Fuel Cells and Corrosion in Solar Energy Systems, Pennington, NJ, Electrochem. Soc. Proc. Ser. (1983) 124–139, PV 83-1.
[12] C.Y. Yuh, J. Colptzer, K. Dickson, M. Farooque, G. Xu, J. Mater. Eng. Perform. 15 (4) (2006) 1–6.
[13] R.A. Donado, L.G. Marianowski, H.C. Maru, J.R. Selman, J. Electrochem. Soc. 131 (11) (1984) 2535–2540.
[14] J. Jun, J.H. Jun, K. Kim, J. Power Sources 112 (1) (2002) 153–161.
[15] US Patent, No. US2002/6,372,374 (April 16, 2002).
[16] P. Biedenkopf, M. Bischoff, M. Spiegel, H.J. Grabke, in: J.R. Selman, I. Uchida, H. Wendt, D. Shores, T.F. Fuller (Eds.), Carbonate Fuel Cell Technology IV, Pennington, NJ, Electrochem. Soc. Proc. Ser. (1997) 386–403, PV 97-4.

[17] I. Parezanovic, E. Strauch, M. Spiegel, J. Power Sources 135 (1/2) (2004) 52–61.
[18] P. Biedenkopf, M. Bischoff, T. Wochner, Mater. Corros. 51 (2000) 287–302.
[19] T. Nishina, M. Arai, H. Inomata, C.G. Lee, I. Uchida, T. Shimada, Proceedings of the Second International Fuel Cell Conference, Kobe, Japan, February 5–8, 1996, pp. 185–188.
[20] L. Jian, C.Y. Yuh, M. Farooque, Corros. Sci. 42 (9) (2000) 1573–1585.
[21] K. Ohe, T. Shimada, N. Ariga, K. Masamura, Proceedings of the Second International Fuel Cell Conference, Kobe, Japan, February 5–8, 1996, pp. 181–184.
[22] US Patent, No. US2003/6,645,657 (November 11, 2003).
[23] US Patent Application, No. US2005/0277015 (December 15, 2005).